research articles Journal of proteome research

# Immunoproteomic Identification of Secretory and Subcellular Protein Antigens and Functional Evaluation of the Secretome Fraction of *Mycobacterium immunogenum*, a Newly Recognized Species of the *Mycobacterium chelonae*–*Mycobacterium abscessus* Group

**Manish K. Gupta, Venkataramanan Subramanian, and Jagjit S. Yadav***

*Microbial Pathogenesis Laboratory, Department of Environmental Health, University of Cincinnati College of Medicine, Cincinnati, Ohio 45267-0056*

**Received November 3, 2008**

*Mycobacterium immunogenum* has been associated with occupational pulmonary disease hypersensitivity pneumonitis (HP). The aim of this study was to identify immunogenic proteins (antigens) in this pathogen as a first step toward understanding its virulence factors and role in HP etiology. Immunoproteomic profiling of secreted and subcellular protein fractions using a combination of two-dimensional electrophoresis (2-DE), immunoblotting, and matrix-assisted laser desorption/ionization-Time of flight (MALDI-TOF) led to the identification of 33 immunoreactive proteins, comprising of 4 secretory, 6 cell wall-associated, 11 membranous, and 12 cytosolic proteins. Of these, eight immunoreactive proteins represented homologues of the known mycobacterial antigens, namely heat shock protein GroEL, antigen 85A, elongation factor Tu (EF-Tu), L-asparaginase, polyketide synthase, PE-PGRS, PPE, and superoxide dismutase (SOD). Global functional search revealed that the remaining 25 novel mycobacterial antigens in *M. immunogenum* showed homology with hypothetical proteins (11 antigens) and other bacterial proteins (14 antigens) with a role in virulence, survival, and/or diverse metabolic functions. To understand immunogenicity of the secretome in *M. immunogenum*, the major protein spot on the secretome 2D-gel (consisting of multiple secretory antigens such as OtsB and CtpA, among others) was eluted and subjected to functional characterization in terms of induction of innate immune response in murine alveolar macrophages. The secretome eluate caused up-regulation of the proinflammatory cytokines TNF-$\alpha$, IL-1$\beta$, IL-6, and IL-18 and down-regulation of the anti-inflammatory cytokine IL-10, implying a potential of the secreted antigens to cause host immune response underlying the *M. immunogenum*-induced lung disease HP. This is the first report on identification of antigens in *M. immunogenum* as well as on the potential of its secretome proteins to induce host response. The identified antigens could have likely roles in virulence and/or diagnosis and serve as potential targets for drug, biocide, and/or vaccine development.

**Keywords:** *Mycobacterium immunogenum* • Immunoproteomics • Antigens • Alveolar macrophages • Immune response

## Introduction

Nontuberculous mycobacteria (NTM) are ubiquitously distributed in the environment,[1,2] and are known to cause pulmonary disease, skin/soft tissue and lymph node infections,[3] and opportunistic infections in immunocompromised patients such as the HIV infected individuals.[4] Certain species of NTM are associated with immune-mediated diseases such as hypersensitivity pneumonitis (HP).[5] HP also known as extrinsic allergic alveolitis (EAA) is an immunological lung disease that is caused by the inhalation of microbial antigens and organic materials. The symptoms include cough, dyspnea, chest tightness, chills, sweating, malaise, fatigue, and headache, among others.[6,7] In metal cutting industries, exposure to the aerosolized metalworking fluid (MWF) contaminated with nontuberculous mycobacteria of the *Mycobacterium chelonae*–*Mycobacterium abscessus* group has been associated with hypersensitivity pneumonitis in machine workers.[6,8–11] Modern water-based metalworking fluids are both synthetic and nonsynthetic and often contain microorganisms and their products[12] along with the biocides applied for their control. In particular, *Mycobacterium immunogenum*, a recently introduced new species in the *M. chelonae*–*M. abscessus* group, has been proposed as the etiological agent of occupational HP in

* To whom correspondence should be addressed. Dr. Jagjit Yadav, Department of Environmental Health, University of Cincinnati College of Medicine, 3223 Eden Avenue, 137 Kettering Laboratory, Cincinnati, OH 45267-0056. Tel, 513-558-4806; fax, 513-558-4397; e-mail, Jagjit.Yadav@uc.edu.

10.1021/pr8009462 CCC: $40.75 



Published on Web 02/11/2009

MWF-exposed workers.[13] It shows overlapping genotypic and biochemical characteristics of *M. abscessus* and *M. chelonae*. Initially, it was reported that only one genotype of *M. immunogenum* occurs in HP-associated metalworking fluids,[14] but our laboratory has reported the occurrence of multiple genotypes.[15,16] *M. immunogenum* induces hypersensitivity pneumonitis-like lung pathology in laboratory mice.[5] High levels of serum antibody against *M. immunogenum* were reported in automobile parts manufacturing workers exposed to the metalworking fluids or those having HP-like symptoms. This mycobacterial species is susceptible to amikacin and clarithromycin but resistant to the majority of the well-known antibiotics like ciprofloxacin, deoxycycline, cefoxitin, turbomycin, and sulfamethoxazole.[17] Like other members of the *M. chelonae*−*M. abscessus* group, this species has also been reported to cause keratitis and myopia-like symptoms and chronic leg ulcers in infected patients.[18,19]

Considering that HP is an immune-mediated disorder caused by the inhaled antigens, there is a need to identify and characterize the causative antigenic proteins in the etiological agent. However, practically nothing is known about the antigens and other virulence factors in *M. immunogenum*. In the postgenomic era, immunoproteomic approach based on 2-DE and mass spectrometry[20] has proved useful in identification of the immunogenic proteins in several pathogenic organisms.[21,22] In this study, we used this approach to identify immunogenic proteins (antigens) in *M. immunogenum*, with a long-term goal to understand its virulence factors, drug targets, and/or targets for immunodiagnosis of the disease and/or exposure assessment. Different subcellular fractions of *M. immunogenum* cells were prepared and resolved by 2-DE. Several immunodominant proteins were identified using immunoblotting coupled with MALDI-TOF analysis.

While the role of whole cells (cell-associated proteome) of *M. immunogenum* in inducing the immune-mediated HP-like lung pathology and immune response in mice has been reported,[12] the significance of its cell-free proteins (secretome) in this context is unknown. Alveolar macrophages (AMs) which act as one of the first-line defenses against the inhaled mycobacteria have been used as an *ex vivo* cell model to study the host innate immune response against mycobacterial secretory proteins. Considering this and the fact that *M. immunogenum*-exposed murine lungs showed AM infiltration,[5] this immune cell type seemed appropriate for testing the functional significance of secreted proteins (secretome) of *M. immunogenum*. Hence, the major secretome protein fraction eluted from the 2D-gel was investigated for its potential to induce cellular and innate immune responses in alveolar macrophages.

## Materials and Methods

**Bacterial Strains and Antibody Probe.** *M. immunogenum* (ATCC 700506), an original isolate from HP-linked metal working fluids,[17] was used. It was routinely maintained on Middlebrook 7H10 enrichment agar at 37 °C. A polyclonal antibody against *M. immunogenum* was custom-raised (Proteintech, Inc., Chicago, IL) in rabbit using heat-inactivated whole cell suspension.

**Preparation of Secretory and Subcellular Protein Fractions.** *M. immunogenum* cells grown in Sauton's medium up to midlog phase were harvested by centrifugation at 12 000*g* and washed twice with 10 mM Tris-HCl (pH 7.5). The cells were then resuspended in 10 mM Tris-HCl (pH 7.5) containing protease inhibitor cocktail (Sigma, St. Louis, MO) and lysed by sonication using 5 cycles of alternate 30 s pulsing and 30 s chilling on ice. Different subcellular fractions (cytosolic, cell wall, cell membrane) were prepared by differential centrifugation as reported earlier.[23] The cell wall fraction and the membrane fraction were washed and resuspended in 10 mM Tris-HCl (pH 7.5) and ammonium bicarbonate buffer (100 mM, pH 8.6), respectively. A homogeneous suspension of the membrane fraction was obtained by incubating it in a water bath sonicator and dialyzing in ammonium bicarbonate buffer containing 10 mM dithiothreitol (DTT). The secretory proteins (secretome) fraction was prepared by filtration (0.22 $\mu$m) and trichloroacetic acid (TCA) precipitation[24] of the culture supernatant followed by resuspension of the precipitate in rehydration buffer (9 M urea, 2 M thiourea, 4% 3-[(3-cholamidopropyl) dimethyl-amonio]-1propanesulfonate (CHAPS), 65 mM DTT). Protein concentration in different fractions (subcellular and secretory) was determined using the Quick Start Bradford protein assay (Bio-Rad, Hercules, CA) according to the manufacturer's specifications.[25]

**SDS-PAGE and Immunoblotting.** Proteins in the test fraction were resolved by discontinuous SDS-PAGE using 12% polyacrylamide gels (Bio-Rad, Hercules, CA) and detected by Coomassie blue staining (Sigma, St. Louis, MO). A replica gel was subjected to Western blot analysis using the primary antibody (1:200 dilution) for *M. immunogenum* and the commercial (Bio-Rad, Hercules, CA)[26] HRP-conjugated goat anti-rabbit antibody (1:3000 dilution) followed by chemiluminescence detection (Promega, Madison, WI) on an X-ray film (Kodak, Rochester, NY).

**2-DE and Immunoblotting.** Sample for the isoelectric focusing (IEF) step was prepared using 100 $\mu$g of the protein fraction of interest in 125 $\mu$L of rehydration buffer (9 M urea, 2 M thiourea, 4% CHAPS, 65 mM DTT, 0.5% IPG buffer and 0.002% bromophenol blue). The IEF was performed on a 7 cm immobiline dry strip pH 3−10 or pH 4−7 (GE Healthcare, Piscataway, NJ) using a IPGphore II isoelectric focusing system (GE Healthcare, Piscataway, NJ). The strip was rehydrated at 15 °C for 12 h using 50 $\mu$A and focused for 16 000 Vh with an upper current limit of 50 $\mu$A. Prior to running in the second dimension, the strip was incubated twice (10 min each) in equilibration buffer (6 M urea, 30% glycerol, 0.05 M Tris, pH 8.8, 2% SDS, 0.002% bromophenol blue), first with 135 mM DTT and then with 135 mM iodoacetamide. Proteins resolved on the IEF strip were separated in the second dimension using 10% SDS-PAGE. The gels were stained with SYPRO Ruby (Invitrogen, Carlsbad, CA) for imaging. Replica gels run in parallel were blotted onto nitrocellulose membrane using the semidry electroblotter (CBS Scientific, Solana Beach, CA). Western blot analysis was performed using the polyclonal antibody against *M. immunogenum*. The 2D-gel and 2D-immunoblot images were overlaid using the 2D-imaging software (Imagemaster 2D Elitegive version 4.01). The spots showing immunofluorescence were manually picked from the SYPRO Ruby-stained gel with one-touch spot picker (The Gel Co., San Francisco, CA) and prepared for MALDI-TOF analysis. Antiserum from uninfected rabbit was used as a control and no immunogenic proteins were detected on these blots. In a subsequent effort to improve the 2DE-resolution of the secreted proteins, a larger IPG strip (24 cm) and a precast

4−20% gradient gel (Jule, Inc., Milford, CT) were used for the separations.

**Immunoreactive Protein Identification by MALDI-TOF Peptide Mass Mapping.** Immunodominant protein spots on the 2D-gel were excised and chopped into small pieces followed by 3 alternate cycles of washing with 500 $\mu$L of 50% acetonitrile (ACN) in 25 mM ammonium bicarbonate buffer, pH 8.0, and dehydration using 100% ACN. The treated sample was dried completely by vacuum centrifugation followed by rehydration at 4 °C for 1 h with 25 $\mu$L of trypsin digestion buffer (100 mM ammonium bicarbonate buffer containing 1 mM $CaCl_2$) containing 50 ng of trypsin gold (Promega, Madison, WI). Enough buffer without trypsin was then added to completely submerge the gel. The reaction mixture was incubated at 37 °C by continuous shaking for 16 h. Following incubation, the reaction mixture was treated with 50 $\mu$L of 5% trifluoroacetic acid (TFA) in 50% ACN (v/v) for 10 min to extract the protein digest. This process was repeated and the extracts were pooled. The eluted digested protein sample was evaporated by vacuum centrifugation and kept at −20 °C until use. During sample analysis, the peptide extracts were dissolved using 5% TFA in 50% ACN.

The MALDI-TOF analysis was performed using a PE Voyager DE_STR biospectrometry work station (Applied Biosystems, Foster city, CA). The matrix α-cyano-4-hydroxycinnamic acid (CHCA) was prepared in a saturated solution of 50% ACN−0.1% TFA. For the mass spectral analysis, equal volumes of the matrix solution (1 $\mu$L) and the sample (1 $\mu$L) were mixed on the sample plate, and the mixture was air-dried to form crystals. Each peptide mass spectrum was calibrated using external standards from Sigma (Insulin oxide $\beta$, ACTH Fragment, Angiotensin I, Bradykinin) and internally calibrated with trypsin autolysis peaks (monoisotopic peaks of trypsin auto digests were 842.508, 1045.504 and 2211.108 $m/z$).

**Bioinformatic Analysis.** Automated analysis of the mass peaks was done using MASCOT search engine (http://www.matrixscience.com/search_form _select.html) against the protein databases. To assign a positive identification, at least three peptides had to match, with a search tolerance of 100 ppm while allowing one miscleavage; possible fixed modifications ascribed to alkylation of cysteine by carbamidomethylation and oxidation of methionine were taken into consideration. For the peptide mass fingerprinting based identification, a minimum of one significance hit ($P < 0.05$) was considered as an identity. The MASCOT search allowed identification of a 'significant hit' based on a 'mass score' cutoff value returned in the output. In some instances, the protein was identifiable despite the low mass score because its top hit was a mycobacterial protein (which allowed it to be differentiated from other proteins). The bioinformatics approach for protein identification is demonstrated in the Supporting Information showing GroEL protein identification of *M. immunogenum* as an example (supplementary file 1).

**Mycobacterial Database Searching.** The MASCOT identified proteins were characterized using the available mycobacterial databases, namely Tuberculist (www.sanger.ac.uk), Proteome 2D-PAGE Database (http://web.mpiib-berlin.mpg.de/cgi-bin/pdbs/2d-page), and pseudo gel images of mycobacterial proteins (http://cmr.tigr.org/tigr-scripts/CMR/shared/Pseudo2DGel.) and the published literature on mycobacterial proteins.

**Functional Analysis of the Major Secretome Fraction (Secretome Eluate).** 2-DE of the secretome yielded a dominant protein spot consisting of major fraction (almost 99%) of the unresolved secretory proteins; the spot yielded a large immunoreactive signal in the Western blot. This major immunoreactive protein spot was subsequently electroeluted[27] for functional analysis using a freshly run 2D-gel. Total protein concentration in the eluted secretome fraction (also designated as 'secretome eluate') was determined as above. This eluate preparation represented a mixture of immunoreactive proteins of the secretome, some of which were identifiable (see Table 5).

Mouse alveolar macrophage cell line MH-S (ATCC CRL-2019) that possesses characteristics very close to those of the primary AMs was used to study the effect of the secretome eluate in terms of cytokine expression profile and cellular damage. One day prior to stimulation, $5 \times 10^6$ macrophage cells were seeded in each well of a 24-well tissue culture plate containing RPMI medium (1 mL) supplemented with 10% fetal bovine serum (FBS). The adhered cells were stimulated with the test antigen preparation at a final concentration of 5 $\mu$g/mL. MH-S cells treated with the same volume of phosphate buffered saline (negative control) and commercial bacterial lipopolysaccharide LPS (Sigma, St. Louis, MO, Cat. no L-4130) at a concentration of 1 $\mu$g/mL (positive control) were used for comparison. The treated cell cultures were harvested at 4, 24, and 48 h intervals during incubation for monitoring the induction of cytokines and cellular changes (in terms of cell viability, lactate dehydrogenase, nitric oxide, caspase 3).

Viable cell count was determined using Trypan Blue staining method (Gibco, Grand Island, NY). Cytotoxicity was measured based on release of lactate dehydrogenase (LDH) using the CytoTox 96 kit (Promega, Madison, WI), according to the manufacturer's instructions. Nitric oxide (NO) production was measured as nitrite using Griess reagent (Promega, Madison, WI) according to the manufacturer's protocol. The nitrite concentration was calculated as micromolar ($\mu$M) using a $NaNO_2$ standard curve, prepared for the purpose as described previously.[28] Caspase activity was measured using the pro-glow caspase-3/7 assay kit (Promega, Madison, WI) per manufacturer's specifications. All activities were measured using a microtiter plate reader (Wallac Victor$^2$ Multilabel Counter Perkin-Elmer, Waltham, MA).

**RNA Isolation and Cytokine Analysis.** Total RNA was extracted from the macrophage cells using TRI Reagent (Molecular Research Center, Cincinnati, OH), according to the manufacturer's protocol. Expression levels for the individual cytokines IL-1$\beta$, IL-6, IL-10, IL-18, and TNF-α were measured by one-step quantitative real time RT-PCR using Brilliant II SYBR Green QRT-PCR 1-Step Master Mix (Stratagene, Ceder Creek, TX) in ABI 7500 PCR thermal cycler. The reaction conditions for the RT-PCR were as follows: RT reaction at 50 °C for 30 min followed by 40 cycles of PCR amplification (denaturation at 94 °C for 45 s, annealing at 53 °C for 45 s, and extension at 72 °C for 35 s). Sequences of the PCR primers used in this study are listed in Table 1. The reaction mixture contained 5 $\mu$L of the 2× master mix, 0.75 $\mu$L each (15 ng) of the forward and reverse primers, 1 $\mu$L of a 1:40 dilution of the reference dye, one unit of the enzyme, and 100 ng of the extracted RNA. Volume of the reaction mixture was made to 10 $\mu$L using distilled water. Cycle threshold (Ct) values for the cytokines were normalized against $\beta$-actin. The fold change in gene expression was calculated according to the published method[29] using the following formula: Fold-change $= 2^{\Delta\Delta Ct}$, where $Ct$ is the threshold cycle, $\Delta Ct$ is the difference between the $Ct$ values of the target gene and the internal control gene

**Table 1.** List of RT-PCR Primers Used in the Study[a]

| target gene | | primer sequence (5′−3′) |
|---|---|---|
| **IL−1β** | FW | AGTGTGGATCCCAAGCAATACC |
| | RV | ATGGTTTCTTGTGACCCTGAGC |
| **IL−6** | FW | TCACAGAGGATACCACTCCC |
| | RV | GGTACTCAGAAGACCAGAG |
| **IL−10** | FW | TCAGCCAGGTGAAGACTTTC |
| | RV | CACCTTGGTCTTGGAGCTT |
| **IL−18** | FW | TTGGCCGACTTCACTGTAC |
| | RV | TGTGTCCTGGAACACGTTTC |
| **TNF−α** | FW | CCTGTAGCCCACGTCGTAGC |
| | RV | TTGACCTCAGCGCTGAGTTG |
| **β−actin** | FW | CAGCCTTCCTTCTTGGGTATGG |
| | RV | CTCATCGTACTCCTGCTTGCTG |

[a] FW = forward primer; RV = reverse primer.

(β-actin), ΔΔCt represents the difference between the ΔCt value for the vehicle control cells and the treated cells.

**Statistical Analysis.** The functional evaluation data were statistically analyzed and the results are expressed as means ± standard deviation. Significance of the differences among the groups was determined by one-way ANOVA using SPSS (16th version). Significance was accepted at $p \leq 0.05$.

## Results

**Optimization of Separation and Identification of Immunogenic Proteins in *M. immunogenum*.** Multiple immunodominant protein spots were detected in the individual subcellular protein fractions of *M. immunogenum* when analyzed on regular (one-dimensional) SDS-PAGE combined with immunoblotting (data not shown). However, the hybridizing protein spots on the Western blots were too confluent to allow complete resolution of the corresponding individual immunogenic proteins for further identification. Hence, for better resolution to allow definitive identification of each of these proteins, the protein fractions were resolved on 2D-gels using immobiline dry IEF strips (GE Healthcare, Piscataway, NJ). For initial standardization purposes, proteins in the test fractions were separated on 7 cm IEF strips with a pH range of 3−10 before separation in the second dimension using SDS-PAGE. Most of the proteins were found clustered around the 4−7 pH range. Hence, our further proteomic separations were performed using IEF strips of pH range 4−7. Up to 300 distinct protein spots were visualized in the second-dimension gel (SDS-PAGE) for each protein fraction (cytosolic, cell membrane, cell wall, and secretory) (Figure 1A−D). Over 50 protein spots from different fractions showed distinct immunoreactivity on the Western blots (Figure 2). Of these, 33 were conclusively identified based on mass peak profiling of the tryptic-digested peptides using MALDI-TOF. MASCOT search results on the identified proteins are presented in Tables 2−5.

**Mycobacterial Antigen Homologues.** Of the identified 33 immunogenic proteins, the following eight proteins showed homology with the known protein antigens reported in other species of mycobacteria: heat shock protein GroEL (60 kDa chaperonin 2), glycine-rich proteins PE-PGRS and PPE, L-asparaginase, polyketide synthase (PKS), antigen 85A (Ag85A), superoxide dismutase (SOD), and elongation factor Tu (EF-Tu).

**Novel Mycobacterial Antigens.** The other 25 of the 33 identified immunogenic proteins represented novel mycobacterial antigens. The majority of these 25 immunogenic proteins along with the 8 antigen homologues listed above could be categorized as those involved in the following biological functions (Figure 3): cell division (protein kinase G designated as PknG), stress (chaperonic heat shock protein GroEL, superoxide dismutase), cation transportation (CtpA), proton transportation (ATP synthase subunits alpha, beta, and delta), fatty acid metabolism (fatty acid CoA ligase, polyketide synthase), DNA replication (ATP-dependent helicase), DNA repair (RecD), biosynthesis of different cell components (UDP-*N*-acetylmuramoylalanyl-D-glutamate-2, trehalose-6-phosphate phosphatase OtsB, molybdopterin biosynthesis protein MoeY, L-Asparaginase, antigen 85A), protein synthesis (aspartate tRNA ligase, EF-Tu), and signal transduction (sensor histidine kinase SenX3, Ser/Thr-protein kinase PknF). The remaining 11 of the 25 immunoreactive proteins showed homology to either unidentified membrane proteins or hypothetical proteins (unannotated) in the mycobacterial database (Figure 3). Interestingly, some of the 25 novel antigen candidates showed homology with virulence factors reported in different pathogenic bacterial species including mycobacteria. For instance, Ser/Thr-protein kinases PknF and PknG[48] have been reported as virulence factors in mycobacteria, but their identity as antigens has not been known.

**Functional Analysis of the Major Secretome Fraction of *M. immunogenum*.** Evaluation of the secretome eluate (the major secretome fraction eluted from the 2D-gel) for its interactions with alveolar macrophages is presented in Figures 4 and 5. In this context, expression of the cytokines IL-β, IL-6, IL-18, and TNF-α was found to be up-regulated (Figure 4) on stimulation with the secretome eluate and the control antigen (LPS) unlike the expression of IL-10 that showed down-regulation (Figure 4C) in both the test and LPS control assays. Expression of IL-6 peaked at 4 h followed by a gradual decline, whereas that of other cytokines (IL-β, IL-18, TNF-α) showed a gradual increase, peaking at the later stages of incubation (24 or 48 h).

In terms of the cellular effects on the alveolar macrophages as compared to LPS (positive control) and the vehicle (negative control), the secretome eluate caused minimal loss of cell viability (Figure 5B) and marginal induction of caspase 3 expression (Figure 5D) in the secretome-treated macrophages as compared to the vehicle-treated macrophages. In contrast, nitric oxide (NO) production (Figure 5C) and LDH release (Figure 5A) were significantly ($P \leq 0.05$) increased at both 24 and 48 h post-treatment in the secretome-treated macrophages as compared to the vehicle-treated cells.

## Discussion

Immunoproteomic analysis of the secretory and cellular subfractions of *M. immunogenum* proteome led to the identification of 33 antigenic proteins (8 homologues and 25 novel antigens) from an array of more than 50 distinctly immunoreactive spots. Interestingly, a sizable fraction (34%) of the identified antigens matched the unannotated hypothetical proteins in the mycobacterial database representing hitherto unnamed novel proteins (Figure 3). Unlike the subcellular fractions, the secretome fraction did not resolve as efficiently into individual spots in our initial efforts (Figure 1D). Nevertheless, in subsequent efforts during the writing of this report, a better resolution of the secretome proteins was achieved by using further improvements in our meth-

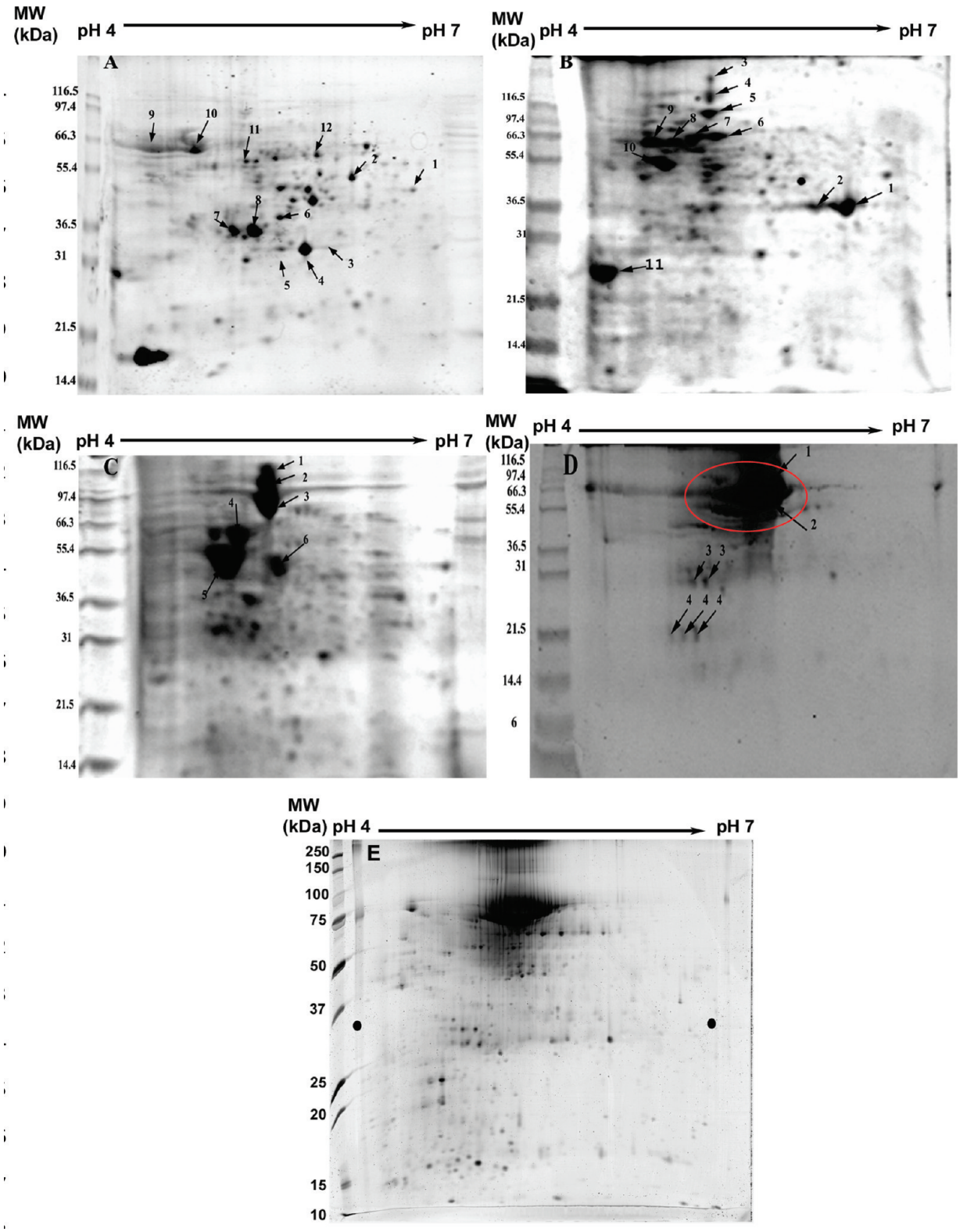


**Figure 1.** Proteomic profiling of the subcellular and secretory protein fractions of *M. immunogenum* 700506. Representative two-dimensional (2D) gel electrophoresis patterns of the different protein fractions: (A) cytosolic fraction; (B) cell membrane fraction; (C) cell wall fraction; (D) secretory fraction. Cells grown to midlog phase in Sauton's medium were extracted to prepare different fractions using differential centrifugation strategy as described under Materials and Methods. An aliquot (100 $\mu$g) of each fraction was subjected to isoelectric focusing (IEF) step, using IPG strip of pH 4−7. Second-dimension separation using SDS-PAGE was done on a 10% acrylamide gel (cytosolic, cell membrane and cell wall fractions) or a 12% acrylamide gel (secretory fraction) and visualized by SYPRO Ruby staining. The spot numbering corresponds to the individual identified proteins listed in Tables 2−5. (E) An improved 2D resolution of the secretory fraction based on use of the modified separation conditions. Briefly, a larger size (24 cm) IPG strip pH 4−7 was used for the IEF step using 400 $\mu$g of protein aliquot of the secretory fraction and a precast 4−20% gradient gel (Jule, Inc., Milford, CT) instead of a linear gel was applied for the second-dimension separation step.

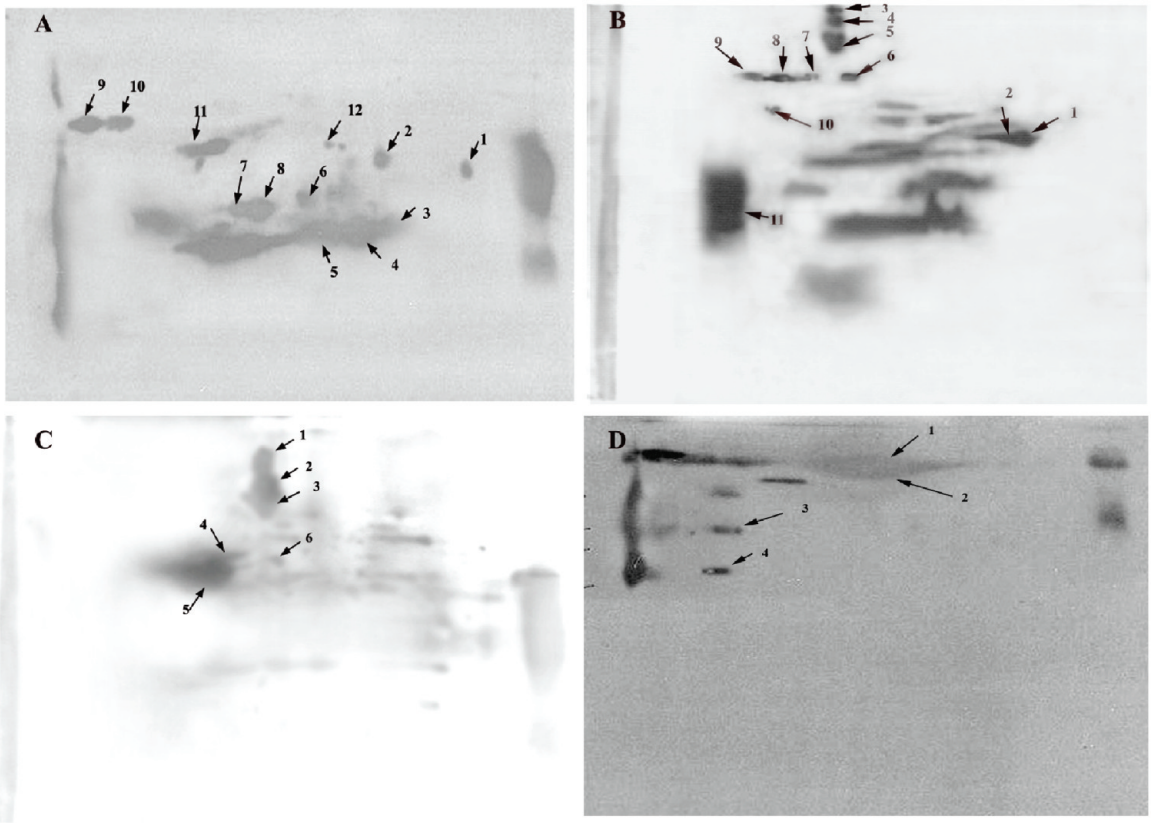


**Figure 2.** Representative 2D-gel immunoblots for individual protein fractions of *M. immunogenum*: cytosolic (A), cell membrane (B), cell wall (C), and secretory (D) fractions. The 2D-gels were run as described in the legend for Figure 1(panels A−D) and blotted onto a nitrocellulose membrane. Western blot analysis was performed using the *M. immunogenum* antibody probe. The immunoreactive protein spot numbers on the blots (panels A−D) correspond to those indicated in the stained replica 2D-gel (Figure 1, panels A−D).

**Table 2.** Cytosolic Antigens of *M. immunogenum*

| spot no. | protein ID | MW/p*I* | sequence coverage (%) | number of mass values matched | mass score | accession no. | putative function(s) |
|---|---|---|---|---|---|---|---|
| 1 | SenX3 | 47967/5.9 | 17.8 | 4 | 25.4 | P54883 | Role in stress signals transduction |
| 2 | ATP synthase subunit alpha | 59289/5.0 | 10.2 | 7 | 35 | P63674 | Important role in proton transport and pH maintenance of cell |
| 3 | Acyl-CoA dehydrogenase | 41720/5.3 | 26 | 4 | 27 | P46703 | Role in transfer of acyl chains directly from carrier proteins to lysine residue |
| 4 | SOD | 22998/5.96 | 33 | 4 | 21 | DQ155691.1 | Catalyzes the conversion of superoxide into oxygen and hydrogen peroxide |
| 5 | Uncharacterized conserved protein | 24571/5.82 | 80 | 18 | 100 | ZP_00878411 | Function not known |
| 6 | Serine/threonine-protein kinase PknF | 50699/5.6 | 14.5 | 4 | 30 | Q7TZN1 | Glucose transport and cell division |
| 7 | Lipoprotein LppW | 33529/ 5.30 | 72 | 22 | 69 | NC_009565.1 | Alanine-rich protein |
| 8 | L-asparaginase | 31721/4.90 | 44 | 14 | 22 | P63627 | Involved in metabolism of asparagine |
| 9 | GroEL or 60 kDa chaperonin 2 | 56892/4.9 | 32 | 14 | 112 | CH602_MYCUA | Heat shock protein in mycobacteria |
| 10 | GroEL or 60 kDa chaperonin 2 | 56643/4.8 | 44.5 | 18 | 99 | P42384 | Heat shock protein in mycobacteria |
| 11 | ATP synthase subunit beta | 53095/4.9 | 26.5 | 9 | 53 | P63678 | Part of $F_1F_o$−ATP synthases |
| 12 | ATP synthase delta chain | 48940/5.1 | 23.5 | 10 | 48 | P53006 | Part of $F_1F_o$−ATP synthases |

odology (Figure 1E). Percent distribution of the identified antigens under various functional categories is presented in Figure 3.

**Mycobacterial Antigen Homologues.** Understanding the existing structural and functional information on the known mycobacterial antigens, for which the homologues have been identified in *M. immunogenum*, may likely provide an insight into the physiology of production and likely role of these detected antigen homologues in this newly recognized species. For instance, heat shock protein GroEL, also referred to as HSP60 or 65-kDa antigen or 60 kDa chaperonin 2, has been reported as a common stress protein[30,31] expressed in response to heat shock in mycobacteria. It is up-regulated in the intracellular postphagocytosis environment as compared to the *in vitro* growth conditions.

SOD plays an important role in conversion of oxygen free radical superoxide ($O_2^-$) to hydrogen peroxide and molecular oxygen.[32,33] It protects mycobacteria from oxidative stress and contributes to their survival and establishment inside the host. This enzyme is extracellularly secreted during growth for combating the protective oxidative stress response of the host.[34,35]

PPE and PE-PGRS belong to the glycine-rich PE (Pro-Glu) and PPE (Pro-Pro-Glu) protein families; these are two multigene families of unknown function, constituting around 10% of the genome in *M. tuberculosis*. The two families are

**Table 3.** Cell Membrane-Associated Antigens of *M. immunogenum*

| spot no. | protein ID | MW/p*I* | sequence coverage (%) | number of mass values matched | mass score | accession no. | putative function(s) |
|---|---|---|---|---|---|---|---|
| 1 | Hypothetical protein Rv3555c | 31836/9.29 | 42 | 8 | 61 | A70604 | Unknown function |
| 2 | Probable oxidoreductase | 32379/8.07 | 21 | 3 | 28 | E70848 | Thiol−disulfide oxidoreductases catalyze formation, disruption, or isomerization of disulfide bonds between cysteine residues in proteins |
| 3 | Probable polyketide synthase | 227175/5.29 | 10 | 13 | 24 | E70522 | Involved in biosynthesis of complex lipids |
| 4 | Cation-transporting ATPase | 167757/5.41 | 9 | 10 | 27 | Q7U2U7 | Acts as an iron transporter in bacterial cells from external environment |
| 5 | Probable MoeY protein | 78133/5.69 | 12 | 7 | 31 | B70741 | Possibly involved in molybdopterin biosynthesis |
| 6 | Probable RecD protein | 61709/6.70 | 23 | 19 | 20 | B70612 | Involved in DNA repair |
| 7 | Long-chain-fatty-acid-CoA ligase, putative | 64321/5.87 | 30 | 17 | 27 | Q7D7D8 | Involved in fatty acid metabolic process |
| 8 | probable pknG protein | 81527/5.51 | 20 | 16 | 26 | H70628 | Serine/threonine protein kinase |
| 9 | PE-PGRS family protein | 68062/4.19 | 10 | 3 | 21 | Q7U0P1 | Structural protein present on the outer surface of mycobacteria cells |
| 10 | Aspartate-tRNA ligase | 65186/5.07 | 21 | 10 | 27 | C70724 | Involved in protein synthesis |
| 11 | PPE family protein | 24346/4.83 | 22 | 3 | 23 | YP_001288073 | Involved in antigenic variation |

**Table 4.** Cell Wall-Associated Antigens in *M. immunogenum*

| spot no. | protein ID | MW/p*I* | sequence coverage (%) | number of mass values matched | mass score | accession no. | putative function(s) |
|---|---|---|---|---|---|---|---|
| 1 | Probable UDP-*N*-acetylmuramoylalanyl-D-glutamate-2 | 55307/6.29 | 18 | 4 | 23 | B70580 | Catalyzes peptide bond formation between UDP *N*-acetylmuramoyl-l-alanine and D-glutamate |
| 2 | Probable UDP-*N*-acetylmuramoylalanyl-D-glutamate-2 | 55307/6.29 | 13 | 3 | 21 | B70580 | Same as above |
| 3 | Probable UDP-*N*-acetylmuramoylalanyl-D-glutamate-2 | 55307/6.29 | 23 | 5 | 34 | B70580 | Same as above |
| 4 | Hypothetical protein Rv1165 | 67709/5.51 | 15 | 5 | 31 | F70556 | Unknown function |
| 5 | Possible conserved membrane protein | 61031/5.72 | 34 | 8 | 70 | Q7TVE7 | Unknown function |
| 6 | ATP-dependent DNA helicase | 59779/ 5.73 | 23 | 7 | 36 | Q8VKC6 | ATP-dependent DNA helicase activity |

**Table 5.** Secretory Protein Antigens in *M. immunogenum*

| spot no. | protein ID | MW/p*I* | sequence coverage (%) | number of mass values matched | mass score | NCBI accession no. | putative function(s) |
|---|---|---|---|---|---|---|---|
| 1[a] | OtsB protein | 145694/5.86 | 8 | 6 | 27 | D70759 | Involved in trehalose biosynthesis pathways |
| 2[a] | CtpA protein | 79314/6.69 | 14 | 5 | 52 | D70750 | Copper transporting P-type ATPase (CtpA) |
| 3 | Probable iron-regulated elongation factor EF-TU | 43561/5.1 | 20 | 4 | 30 | A5U071 | Has GTPase activity and is involved in protein synthesis |
| 4 | Antigen 85A, mycolyltransferase | 35686/6.5 | 20 | 4 | 45 | Q847N5 | Part of the antigen 85 complex involved in the synthesis of α,α′-trehalose manomycolate(TMM) and α,α′-trehalose dimycolate (TDM) |

[a] These antigens were identified from the major protein spot on the secretome 2D-gel that was used for functional analysis

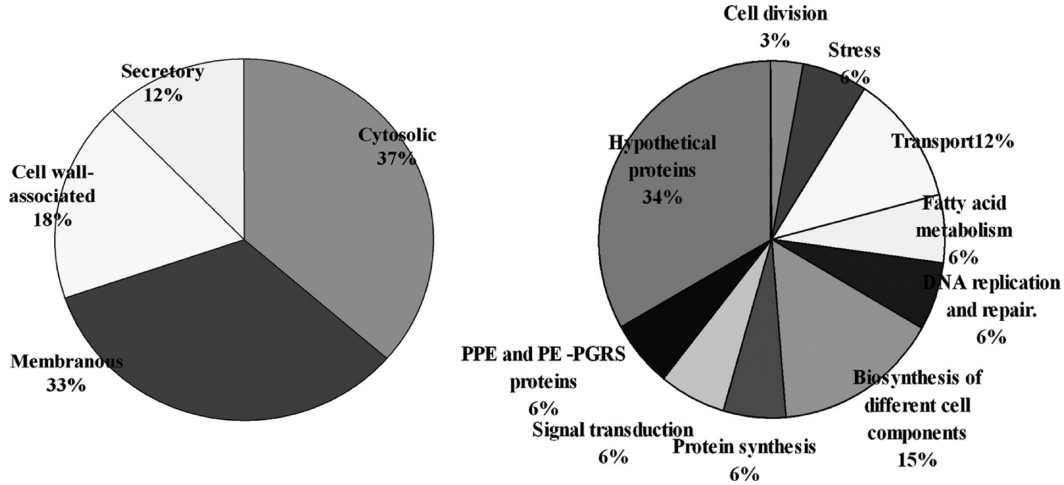


**Figure 3.** Cellular and functional distribution of the identified 33 antigens in *M. immunogenum*. (Left) Percent distribution of the identified antigens in different subcellular fractions and the secretome; (Right) functional clustering of the identified individual antigens.

represented by 100 and 70 member genes, respectively, in the genome of the laboratory strain H37Rv and are the likely source of antigenic variation in the mycobacterial genome. Several members of these glycine-rich multigene protein families are either expressed upon infection of macrophages or when grown under low pH and stress conditions.[36]

Antigen 85A is a member of the antigen 85 complex that comprises of three closely related extracellularly secreted enzymes, antigen 85A, antigen 85B and antigen 85C, with demonstrated immunogenicity. Antigen 85 complex has a role in mycolyl-transferase activity and helps in the formation of cell wall.[37]

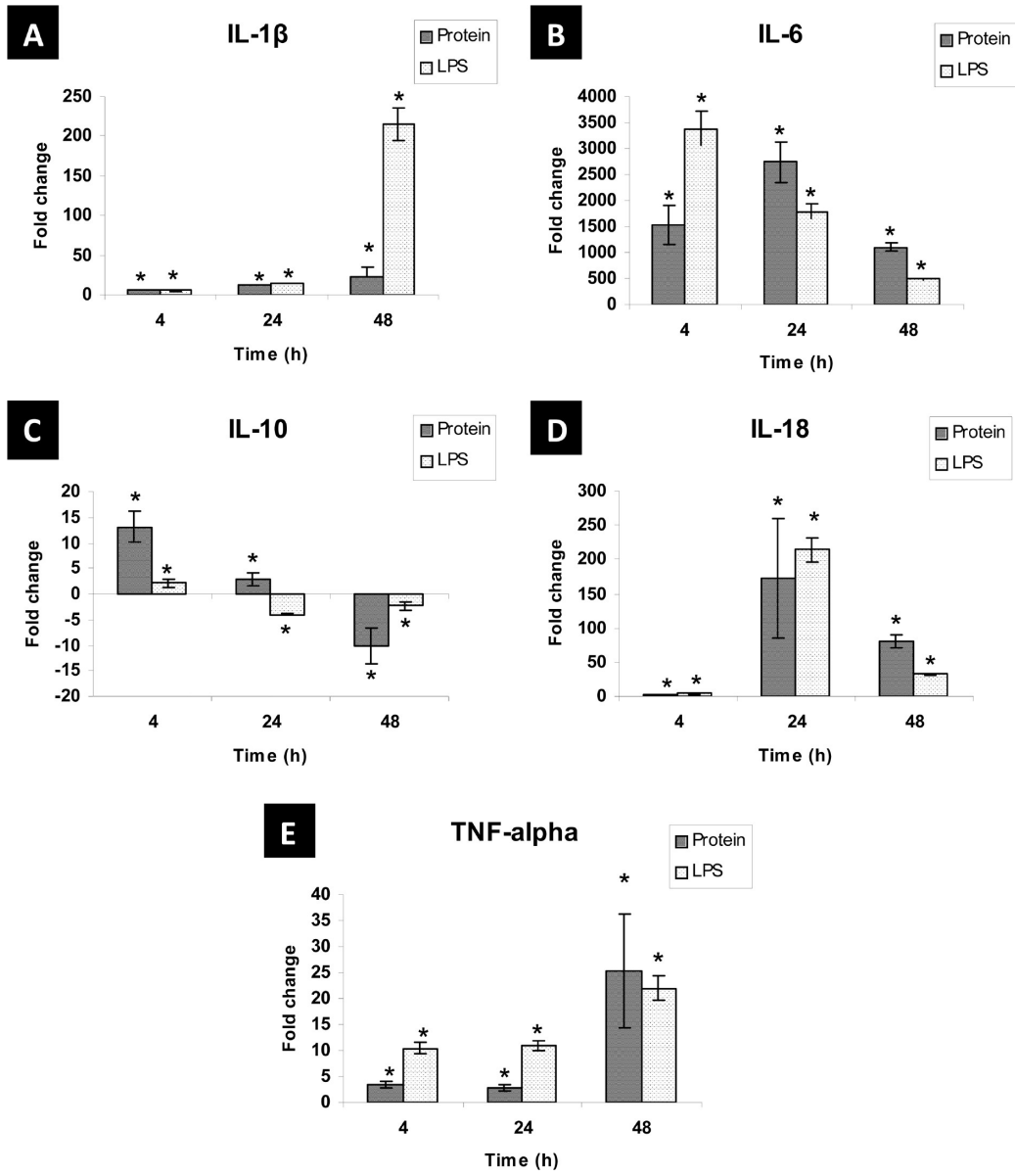


**Figure 4.** Cytokine induction profile in murine alveolar macrophage cells (MH-S cell line) exposed to the secretome eluate of *M. immunogenum* 700506 in a time-course treatment. The following cytokines were measured: (A) IL-1$\beta$, (B) IL-6, (C) IL-10, (D) IL-18, (E) TNF-$\alpha$. Change in cytokine expression was measured by quantitative real time RT-PCR and calculated as fold-change in gene expression relative to $\beta$-actin using the $2^{\Delta\Delta CT}$ method as described in Material and Methods. Mean fold-change in gene expression from the triplicates is plotted on the *Y*-axis. Treatments of MH-S cells with a commercial bacterial lipopolysaccharide, LPS (1 $\mu$g/mL) and the vehicle (PBS) were used as positive and negative controls, respectively, for comparison. Statistical significance ($P \leq 0.05$) of the fold-change data is indicated by an asterisk (*).

Elongation factor Tu (EF-Tu) belongs to a superfamily of GTP-binding proteins that have GTPase activity. It is known to form a complex with aminoacyl-tRNA and elongation factor Ts (EF-Ts), bind with the ribosomes, and help in protein synthesis.[38] Young and co-workers[39] proposed a nutrient-dependent methylation of EF-Tu in *Escherichia coli*, with a role in regulation of growth.

Polyketide synthases are involved in the synthesis of long-chain alpha-pyrones that are components of the complex lipid-rich mycobacterial cell wall. These complex lipids are formed by the combined action of fatty acid synthase and polyketide synthase.[40]

L-asparaginase catalyzes the conversion of L-asparagine into L-asparatate and ammonia. It is expressed intracellularly in the stationary cultures of *Mycobacterium phlei* and other mycobacterial species grown in Sauton's medium or salts-gluconase-glutamate medium.[41] In some bacterial species, it is secreted out into the culture medium.[42]

**Novel Antigens.** Over half of the novel antigens matched other mycobacterial or bacterial proteins known to be involved in different cellular functions such as lipid transport and metabolism, ion transport, protein synthesis, energy production, biosynthesis and modification of cell wall components, cellular structure, transport and metabolism of amino acids, cell signaling, and virulence. For instance, SenX3 is a part of the mycobacterial SenX3−RegX3 two-component system.[43] It helps in the transduction of different stress signals inside the cell. Cytosolic portion of the protein autophosphorylates before

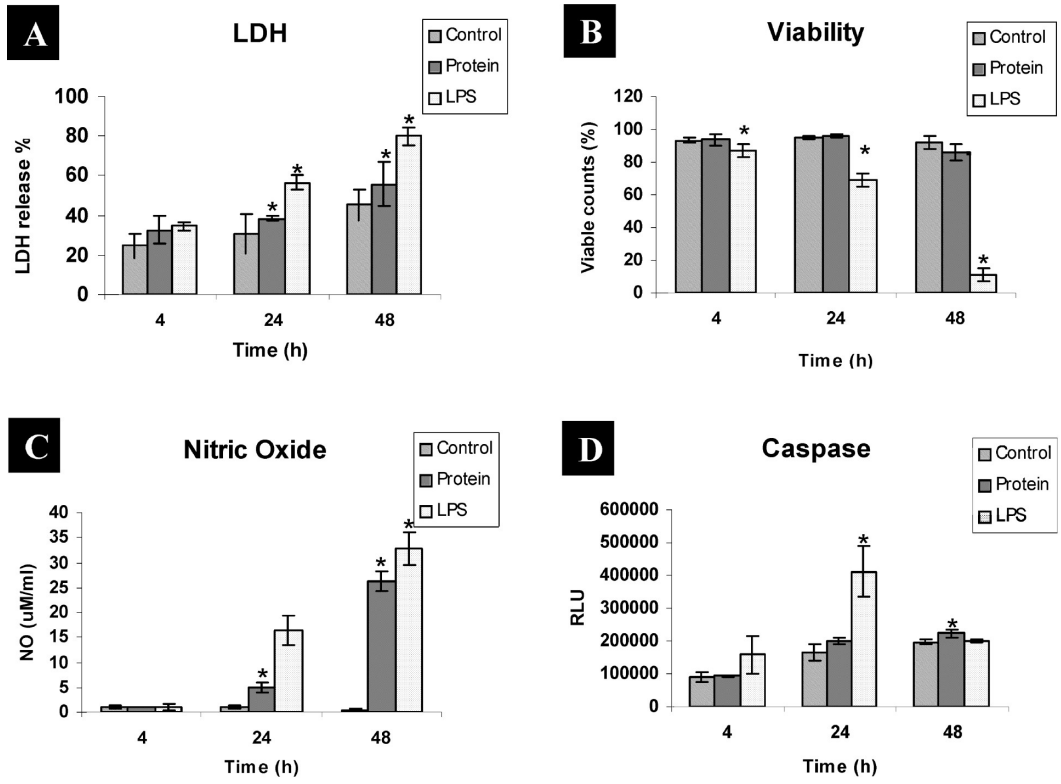


**Figure 5.** Cellular and biochemical effects of the major secretome eluate of *M. immunogenum* toward murine alveolar macrophages (MH-S cell line) in a time-course treatment. (A) Cytotoxicity as measured in terms of induction of lactate dehydrogenase (LDH) release; (B) loss of cell viability as determined by trypan blue dye exclusion method; (C) nitric oxide (NO) production, (D) Caspase 3/7 activation measured as relative luminescence unit (RLU). Treatment of the MH-S cells with LPS (1 $\mu$g/mL) was used as a positive control for comparison. The treatments using the secretome antigen eluate (5 $\mu$g/mL) and LPS (1 $\mu$g/mL) were performed as described in the Materials and Methods. Asterisk on the bar indicates statistical significance ($P \leq 0.05$) of the value with respect to the value of the vehicle-treated control group.

mediating phosphorylation of the response regulator protein RegX3.[43] This protein has a crucial role in survival of bacteria inside the macrophage as well as in the *in vivo* environment.[44] The two-component system (SenX3−RegX3) also regulates the gene expression in mycobacteria in a phosphate-dependent manner.[45]

Detection of protein kinase F (PknF) in *M. immunogenum*, a rapidly growing mycobacterial species, is interesting considering that this protein has been previously reported to occur in the member species of slow-growing mycobacteria (SGM) but not in rapidly growing mycobacteria species (RGM) such as *Mycobacterium smegmatis*. It is a transmembrane protein that has been shown to play a role in the regulation of glucose transport, cell growth, and septum formation in *Mycobacterium tuberculosis*.[46,47] Protein kinase G (pknG) is an important drug target in mycobacteria. This protein is secreted by the pathogenic mycobacterial species inside the phagosome compartment of macrophages. It inhibits phagosome-lysosome fusion and helps in intracellular survival of the pathogenic mycobacteria.[48]

Three subunits (alpha, beta and delta) of $F_1F_0$-ATP synthase were detected in our analysis on *M. immunogenum*. $F_1F_0$-ATP synthase complex plays an important role in various cellular processes in bacterial cells.[11,49] This system is a potent drug target in *M. tuberculosis*, which can be inhibited by diarylquinoline.[50,51] With the use of a knockout mutation of the beta subunit of $F_1F_o$-ATP synthase, it has been demonstrated that this protein is essential for the growth of *M. smegmatis* on fermentable and nonfermentable carbon sources.[52] Acyl-CoA dehydrogenase is a flavoprotein which catalyzes the desaturation of acyl-CoA esters and plays an important role in the oxidation of fatty acyl-CoA esters.[53]

Lipoprotein LppW is an alanine-rich protein that was recently reported from the culture filtrate of *M. tuberculosis*.[54]

UDP-*N*-acetylmuramoylalanyl-D-glutamate catalyzes peptide bond formation between UDP *N*-acetylmuramoyl-L-alanine and D-glutamate.[55] Long chain fatty acid-CoA ligases share homology with the protein fatty acid-CoA ligase FadD which is involved in the synthesis of complex lipids in mycobacteria. These complex lipids are present on the cell surface of pathogenic mycobacteria and play an important role in their virulence mechanisms.[56] Trehalose-6-phosphate phosphatase OtsB (osmoregulatory trehalose synthesis B) is involved in the synthesis of trehalose from glucose-6-phosphate and UDP-glucose through the OtsA−OtsB pathway.[57,58] This protein is up-regulated under stress conditions in *E. coli*.[59] Other mycobacteria species are also known to have homologues of OtsA and OtsB; their activity was demonstrated in the cell-free extracts of *M. smegmatis* and *M. bovis* BCG.[60] OtsA-OtsB pathway is crucial for the growth of *M. smegmatis* as shown by the OtsA mutants that were unable to proliferate and enter the stationary phase.[61]

**Immunogenicity of the Secretome Proteins of *M. immunogenum*.** For immune response studies, the secretome eluate (containing a mixture of major secretory proteins) was used instead of the individual secreted proteins, for two reasons, to

test whether the secretome proteins of *M. immunogenum* as a whole have a role in inducing host innate immune response, and to perform a reliable immunogenicity assay, considering the insufficient concentration and poor resolution of the few individual protein spots. Use of alveolar macrophages as the immune cell type for this analysis is consistent with the established practice in mycobacterial immune response studies.[62−64] The cytokine expression patterns of the secretome-treated macrophage cells were comparable with those of the LPS-treated cells; proinflammatory cytokines (IL-1$\beta$, IL-6, IL-18 and TNF-$\alpha$) were up-regulated, whereas the antiproinflammatory cytokine IL-10 was down-regulated. Our LPS results corroborated with the previous observations that expression of IL-6 is greater than the other proinflammatory cytokines (TNF-$\alpha$ and IL-1$\beta$) in LPS-treated cells,[65] providing authenticity to the experimental conditions used and the patterns of cytokine expression observed in this study. Up-regulation of TNF-$\alpha$ in the treated alveolar macrophages is consistent with a similar immunological response reported for the other antigenic secretory proteins such as Ag 85B and ESAT6 from other species of mycobacteria.[63,66,67] The ability of the secretome proteins of *M. immunogenum* to induce the observed cytokine patterns implies their likely role in inducing inflammation. Additionally, one could expect other specific roles of these proteins attributable to the induced cytokines TNF-$\alpha$,[68−72] IL-1,[73−75] IL-6,[76−79] IL-18[68,80−82] as observed in studies on mycobacterial pathogenesis using other species.

**Cellular Effects of the Secretome Proteins of *M. immunogenum*.** While the secretome eluate proteins caused minimal change in macrophage cell viability, the cells showed some cytotoxicity and the nitric oxide (NO) production was significantly increased. Considering that NO is produced due to the activity of inducible nitric oxide synthase (iNOS) in inflammatory macrophages,[72−83] it is likely that the secretory antigens may have caused iNOS-mediated up-regulation of NO.

Proinflammatory cytokines and nitric oxide induced by the secretory proteins of *M. immunogenum* may be the likely contributing factors to hypersensitivity pneumonitis-like symptoms in the industrial workers exposed to this pathogen. However, further detailed studies are needed to confirm this hypothesis.

## Conclusions

This is the first report on identification of individual protein antigens in the nontuberculous mycobacterial species *M. immunogenum*, a species that is receiving increasing attention as an etiological agent of hypersensitivity pneumonitis in machine workers. The study also provides first evidence on the immunological potential of secretome proteins in this mycobacterial species. Some of the antigen proteins identified in this study are homologues of the potent antigens reported in other species of mycobacteria or in other bacterial species. Particularly, the identified homologues of the two mycobacterial antigens HSP60 and antigen 85A, currently being used in TB diagnosis, could be further characterized to identify *M. immunogenum*-specific epitope(s) for diagnostic applications in hypersensitivity pneumonitis. Importantly, this study has led to the identification of novel antigenic proteins showing homology either with other functional proteins in different bacterial pathogens with a role in their virulence or survival under stress conditions, or with hitherto unannotated proteins in the mycobacterial database. Such species-specific antigens identified in this study may pave the way for understanding the immunogenicity and pathogenesis mechanisms of *M. immunogenum* and developing tools for the diagnosis of mycobacterial-HP patients and/or exposed workers in the occupational settings. Similar applications are expected in nosocomial infections with this species.

**Acknowledgment.** This study was supported by the grant 2R01OH007364 (to J.S.Y.) from the National Institute of Occupational Safety and Health, Center for Disease Control and Prevention. The authors acknowledge Drs. George Smulian and Francisco Gomez of the university's V.A Hospital and Medical Center for their help in MALDI-TOF analysis and Dr. Ying Wai Lam for help in 2D-gel image analysis.

**Supporting Information Available:** Supplementary File 1 provides further information on the bioinformatic analysis methodology used for protein identification (using GroEL protein as an example). This material is available free of charge via the Internet at http://pubs.acs.org.

## References

(1) Falkinham, J. O., III. Nontuberculous mycobacteria in the environment. *Clin. Chest. Med.* **2002**, *23* (3), 529–551.
(2) Von Reyn, C. F.; Waddell, R. D.; Eaton, T.; Arbeit, R. D.; Maslow, J. N.; Barber, T. W.; Brindle, R. J.; Gilks, C. F.; Lumio, J.; Lahdevirta, J.; Ranki, A.; Dawson, D.; Falkinham, J. O., III. Isolation of *Mycobacterium avium* complex from water in the United States, Finland, Zaire, and Kenya. *J. Clin. Microbiol.* **1993**, *31* (12), 3227–3230.
(3) Griffith, D. E.; Aksamit, T.; Brown-Elliott, B. A.; Catanzaro, A.; Daley, C.; Gordin, Fred; Holland, S. M.; Horsburgh, R.; Huitt, G.; Iademarco, F. I.; Iseman, M.; Olivier, K.; Ruoss, S.; von Reyn, C. F.; Wallace, R. J., Jr.; Winthrop, K. An official ATS/IDSA statement: Diagnosis, treatment, and prevention of nontuberculous mycobacterial diseases. 1993−1996. *Am. J. Respir. Crit. Care* **2007**, *175*, 367–416.
(4) Horsburgh, C. R., Jr.; Selik, R. M. The epidemiology of disseminated nontuberculous mycobacterial infection in the acquired immunodeficiency syndrome (AIDS). *Am. Rev. Respir. Dis.* **1989**, *139* (1), 4–7.
(5) Thorne, P. S.; Adamcakova-Dodd, A.; Kelly, K. M.; O'Neill, M. E.; Duchaine, C. Metalworking fluid with mycobacteria and endotoxin induces hypersensitivity pneumonitis in mice. *Am. J. Respir. Crit. Care Med.* **2006**, *173* (7), 759–768.
(6) Fox, J.; Anderson, H.; Moen, T.; Gruetzmacher, G.; Hanrahan, L.; Fink, J. Metal working fluid-associated hypersensitivity pneumonitis: an outbreak investigation and case-control study. *Am. J. Ind. Med.* **1999**, *35* (1), 58–67.
(7) Kurup, V. P.; Zacharisen, M. C.; Fink1, J. N. Hypersensitivity Pneumonitis. *Indian J. Chest Dis. Allied Sci.* **2006**, *48* (2), 115–128.
(8) Kreiss, K.; Cox-Ganser, J. Metalworking fluid-associated hypersensitivity pneumonitis: a workshop summary. *Am. J. Ind. Med.* **1997**, *32* (4), 423–432.
(9) Weiss, L. P. C. L. R.; Rossmoore, H.; Fink, J.; Harney, J.; Trout, D. Respiratory illness in workers exposed to metal working fluid contaminated with nontuberculous mycobacteria -Ohio 2001. *Morb. Mortal. Wkly. Rep.* **2002**, *51*, 349–352.
(10) Anonymous, Biopsy-confirmed hypersensitivity pneumonitis in automobile production workers exposed to metalworking fluids—Michigan, 1994−1995; Jul 19, **1996**; pp 606−610.
(11) Senior, A. E.; Nadanaciva, S.; Weber, J. The molecular mechanism of ATP synthesis by F1F0-ATP synthase. *Biochim. Biophys. Acta* **2002**, *1553*, 188–211.
(12) Thorne, P. S.; Sprince, N. L. Metal working fluids. In *Textbook of Clinical Occupational and Environmental Health*; Resenstock, M. C., Brodkin, C. A., Redlich, C., Eds.; W.B. Saunders: Philadelphia, PA, 2004; pp 43.41−43.12.
(13) Trout, D.; Weissman, D. N.; Lewis, D.; Brundage, R. A.; Franzblau, A.; Remick, D. Evaluation of hypersensitivity pneumonitis among workers exposed to metal removal fluids. *Appl. Occup. Environ. Hyg.* **2003**, *18* (11), 953–960.
(14) Wallace, R. J., Jr.; Zhang, Y.; Wilson, R. W.; Mann, L.; Rossmoore, H. Presence of a single genotype of the newly described species *Mycobacterium immunogenum* in industrial metalworking fluids

associated with hypersensitivity pneumonitis. *Appl. Environ. Microbiol.* **2002**, *68* (11), 5580–5584.
(15) Yadav, J. S.; Khan, I. U.; Fakhari, F.; Soellner, M. B. DNA-based methodologies for rapid detection, quantification, and species- or strain-level identification of respiratory pathogens (Mycobacteria and Pseudomonads) in metalworking fluids. *Appl. Occup. Environ. Hyg.* **2003**, *18* (11), 966–975.
(16) Khan, I. U.; Selvaraju, S. B.; Yadav, J. S. Occurrence and characterization of multiple novel genotypes of *Mycobacterium immunogenum* and *Mycobacterium chelonae* in metalworking fluids. *FEMS Microbiol. Ecol.* **2005**, *54* (3), 329–338.
(17) Wilson, R. W.; Steingrube, V. A.; Bottger, E. C.; Springer, B.; Brown-Elliott, B. A.; Vincent, V.; Jost, K. C., Jr.; Zhang, Y.; Garcia, M. J.; Chiu, S. H.; Onyi, G. O.; Rossmoore, H.; Nash, D. R.; Wallace, R. J., Jr. *Mycobacterium immunogenum* sp. nov., a novel species related to *Mycobacterium abscessus* and associated with clinical disease, pseudo-outbreaks and contaminated metalworking fluids: an international cooperative study on mycobacterial taxonomy. *Int. J. Syst. Evol. Microbiol.* **2001**, *51* (5), 1751–1764.
(18) Sampaio, J. L.; Junior, D. N.; de Freitas, D.; Hofling-Lima, A. L.; Miyashiro, K.; Alberto, F. L.; Leao, S. C. An outbreak of keratitis caused by *Mycobacterium immunogenum*. *J. Clin. Microbiol.* **2006**, *44* (9), 3201–3207.
(19) Loots, M. A.; de Jong, M. D.; van Soolingen, D.; Wetsteyn, J. C.; Faber, W. R. Chronic leg ulcer caused by *Mycobacterium immunogenum*. *J. Travel Med.* **2005**, *12* (6), 347–349.
(20) Rosenkrands, I.; King, A.; Weldingh, K.; Moniatte, M.; Moertz, E.; Andersen, P. Towards the proteome of *Mycobacterium tuberculosis*. *Electrophoresis* **2000**, *21* (17), 3740–3756.
(21) Shin, G. W.; Palaksha, K. J.; Kim, Y. R.; Nho, S. W.; Kim, S.; Heo, G. J.; Park, S. C.; Jung, T. S. Application of immunoproteomics in developing a *Streptococcus iniae* vaccine for olive flounder (Paralichthys olivaceus). *J. Chromatogr., B: Anal. Technol. Biomed. Life Sci.* **2007**, *849* (1−2), 315–322.
(22) Sinha, S.; Kosalai, K.; Arora, S.; Namane, A.; Sharma, P.; Gaikwad, A. N.; Brodin, P.; Cole, S. T. Immunogenic membrane-associated proteins of *Mycobacterium tuberculosis* revealed by proteomics. *Microbiology* **2005**, *151* (7), 2411–2449.
(23) Dahl, J. L.; Wei, J.; Moulder, J. W.; Laal, S.; Friedman, R. L. Subcellular Localization of the Intracellular Survival-Enhancing Eis Protein of *Mycobacterium tuberculosis*. *Infect. Immun.* **2001**, *69* (7), 4295–302.
(24) Gazdik, M. A.; McDonough, K. A. Identification of cyclic AMP-regulated genes in *Mycobacterium tuberculosis* complex bacteria under low-oxygen conditions. *J. Bacteriol.* **2005**, *187* (8), 2681–2692.
(25) Bradford, M. M. A rapid and sensitive method for the quantitation of microgram quantities of protein utilizing the principle of protein-dye binding. *Anal. Biochem.* **1976**, *72* (1−2), 248–254.
(26) Towbin, H.; Staehelin, T.; Gordon, J. Electrophoretic transfer of proteins from polyacrylamide gels to nitrocellulose sheets: procedure and some applications. *Proc. Natl. Acad. Sci. U.S.A.* **1979**, *76* (9), 4350–4.
(27) Lei, Z.; Anand, A.; Mysore, K. S.; Sumner, L. W. Electroelution of intact proteins from SDS-PAGE gels and their subsequent MALDI-TOF MS analysis. *Methods Mol. Biol.* **2007**, *355*, 353–63.
(28) Wang, H.; Yadav, J. S. DNA damage, redox changes, and associated stress- inducible signaling events underlying the apoptosis and cytotoxicity in murine alveolar macrophage cell line MH-S by methanol-extracted Stachybotrys chartarum toxins. *Toxicol. Appl. Pharmacol.* **2006**, *214* (3), 297–308.
(29) Chang, J. T.; Chen, I. H.; Liao, C. T.; Wang, H. M.; Hsu, Y. M.; Hung, K. F.; Lin, C. J.; Hsieh, L. L.; Cheng, A. A reverse transcription comparative real-time PCR method for quantitative detection of angiogenic growth factors in head and neck cancer patients. *J. Clin. Biochem.* **2002**, *35* (8), 591–596.
(30) Alavi, M. R.; Affronti, L. F. Induction of mycobacterial proteins during phagocytosis and heat shock: a time interval analysis. *J. Leukocyte Biol.* **1994**, *55* (5), 633–641.
(31) Monahan, I. M.; Betts, J.; Banerjee, D. K.; Butcher, P. D. Differential expression of mycobacterial proteins following phagocytosis by macrophages. *Microbiology* **2001**, *147* (2), 459–471.
(32) Fridovich, I. Superoxide radical and superoxide dismutase. *Annu. Rev. Biochem.* **1995**, *64*, 97–112.
(33) Hassan, H. M. Mirobial superoxide dismutase. *Adv. Genet.* **1989**, *26*, 65–97.
(34) Dussurget, O.; Stewart, G.; Neyrolles, O.; Pescher, P.; Young, D.; Marchal, G. Role of *Mycobacterium tuberculosis* copper-zinc superoxide dismutase. *Infect. Immun.* **2001**, *69* (1), 529–533.
(35) Liu, X.; Feng, Z.; Harris, N. B.; Cirillo, J. D.; Bercovier, H.; Barletta, R. G. Identification of a secreted superoxide dismutase in *Mycobacterium avium* subsp. paratuberculosis. *FEMS Microbiol. Lett.* **2001**, *202* (2), 233–238.
(36) Ramakrishnan, L.; Federspiel, N. A.; Falkow, S. Granuloma-specific expression of mycobacterium virulence proteins from the glycine-rich PE-PGRS family. *Science* **2000**, *288* (5470), 1436–1439.
(37) Belisle, J. T.; Vissa, V. D.; Sievert, T.; Takayama, K.; Brennan, P. J.; Besra, G. S. Role of the major antigen of *Mycobacterium tuberculosis* in cell wall biogenesis. *Science* **1997**, *276* (5317), 1420–1422.
(38) Sanderova, H.; Jonak, J. Opposite roles of domains 2 + 3 of *Escherichia coli* EF-Tu and Bacillus stearothermophilus EF-Tu in the regulation of EF-Tu GTPase activity. *Biochim. Biophys. Acta* **2005**, *1752* (1), 11–7.
(39) Young, C. C.; Bernlohr, R. W. Elongation factor Tu is methylated in response to nutrient deprivation in *Escherichia coli*. *J. Bacteriol.* **1991**, *173* (10), 3096–3100.
(40) Saxena, P.; Yadav, G.; Mohanty, D.; Gokhale, R. S. A new family of type III polyketide synthases in *Mycobacterium tuberculosis*. *J. Biol. Chem.* **2003**, *278* (45), 44780–44790.
(41) Andrejew, A.; Orfanelli, M. T.; Desbordes. Asparagine metabolism in mycobacteria. I. Comparison of L-asparaginases obtained from BCG, *M. fortuitum* and *M. phlei* (author's transl). *Ann. Microbiol. (Paris)* **1974**, *125A* (3), 323–339.
(42) Dunlop, P. C.; Meyer, G. M.; Ban, D.; Roon, R. J. Characterization of two forms of asparaginase in *Saccharomyces cerevisiae*. *J. Biol. Chem.* **1978**, *253* (4), 1297–1304.
(43) Himpens, S.; Locht, C.; Supply, P. Molecular characterization of the mycobacterial SenX3-RegX3 two-component system: evidence for autoregulation. *Microbiology* **2000**, *146* (12), 3091–3098.
(44) Parish, T.; Smith, D. A.; Roberts, G.; Betts, J.; Stoker, N. G. The senX3-regX3 two-component regulatory system of *Mycobacterium tuberculosis* is required for virulence. *Microbiology* **2003**, *149* (6), 1423–1435.
(45) Glover, R. T.; Kriakov, J.; Garforth, S. J.; Baughn, A. D.; Jacobs, W. R., Jr. The two-component regulatory system senX3-regX3 regulates phosphate-dependent gene expression in *Mycobacterium smegmatis*. *J. Bacteriol.* **2007**, *189* (15), 5495–5503.
(46) Koul, A.; Choidas, A.; Tyagi, A. K.; Drlica, K.; Singh, Y.; Ullrich, A. Serine/threonine protein kinases PknF and PknG of *Mycobacterium tuberculosis*: characterization and localization. *Microbiology* **2001**, *147* (8), 2307–2314.
(47) Deol, P.; Vohra, R.; Saini, A. K.; Singh, A.; Chandra, H.; Chopra, P.; Das, T. K.; Tyagi, A. K.; Singh, Y. Role of *Mycobacterium tuberculosis* Ser/Thr kinase PknF: implications in glucose transport and cell division. *J. Bacteriol.* **2005**, *187* (10), 3415–3420.
(48) Walburger, A.; Koul, A.; Ferrari, G.; Nguyen, L.; Prescianotto-Baschong, C.; Huygen, K.; Klebl, B.; Thompson, C.; Bacher, G.; Pieters, J. Protein kinase G from pathogenic mycobacteria promotes survival within macrophages. *Science* **2004**, *304* (5678), 1800–1804.
(49) Boyer, P. D. ATP synthase- a splendid molecular machine. *Annu. Rev. Biochem.* **1997**, *66*, 717–749.
(50) Andries, K.; Verhasselt, P.; Guillemont, J.; Gohlmann, H. W.; Neefs, J. M.; Winkler, H.; Van Gestel, J.; Timmerman, P.; Zhu, M.; Lee, E.; Williams, P.; de Chaffoy, D.; Huitric, E.; Hoffner, S.; Cambau, E.; Truffot-Pernot, C.; Lounis, N.; Jarlier, V. Diarylquinolines target subunit c of mycobacterial ATP synthase. *Science* **2005**, *307* (5707), 223–227.
(51) Koul, A.; Dendouga, N.; Vergauwen, K.; Molenberghs, B.; Vranckx, L.; Willebrords, R.; Ristic, Z.; Lill, H.; Dorange, I.; Guillemont, J.; Bald, D.; Andries, K. Diarylquinolines target subunit c of mycobacterial ATP synthase. *Nat. Chem. Biol.* **2007**, *3* (6), 323–324.
(52) Tran, S. L.; Cook, G. M. The F1Fo-ATP synthase of *Mycobacterium smegmatis* is essential for growth. *J. Bacteriol.* **2005**, *187* (14), 5023–5028.
(53) Mahadevan, U.; Padmanaban, G. Cloning and expression of an acyl-CoA dehydrogenase from *Mycobacterium tuberculosis*. *Biochem. Biophys. Res. Commun.* **1998**, *244* (3), 893–897.
(54) Malen, H.; Berven, F. S.; Fladmark, K. E.; Wiker, H. G. Comprehensive analysis of exported proteins from *Mycobacterium tuberculosis* H37Rv. *Proteomics* **2007**, *7* (10), 1702–1718.
(55) Crick, D. C.; Mahapatra, S.; Brennan, P. J. Biosynthesis of the arabinogalactan-peptidoglycan complex of *Mycobacterium tuberculosis*. *Glycobiology* **2001**, *11* (9), 107R–118R.
(56) Cox, J. S.; Chen, B.; McNeil, M.; Jacobs, W. R., Jr. Complex lipid determines tissue-specific replication of *Mycobacterium tuberculosis* in mice. *Nature* **1999**, *402* (6757), 79–83.
(57) Kaasen, I.; McDougall, J.; Strom, A. R. Analysis of the otsBA operon for osmoregulatory trehalose synthesis in *Escherichia coli* and homology of the OtsA and OtsB proteins to the yeast trehalose-6-phosphate synthase/phosphatase complex. *Gene* **1994**, *145* (1), 9–15.

(58) Kremer, L.; Dover, L. G.; Morehouse, C.; Hitchin, P.; Everett, M.; Morris, H. R.; Dell, A.; Brennan, P. J.; McNeil, M. R.; Flaherty, C.; Duncan, K.; Besra, G. S. Galactan biosynthesis in *Mycobacterium tuberculosis*: Identification of a bifunctional UDP-galactofuranosyltransferase. *J. Biol. Chem.* **2001**, *276* (28), 26430–26440.
(59) Kaasen, I.; Falkenberg, P.; Styrvold, O. B.; Strom, A. R. Molecular cloning and physical mapping of the otsBA genes, which encode the osmoregulatory trehalose pathway of *Escherichia coli*: evidence that transcription is activated by katF (AppR). *J. Bacteriol.* **1992**, *174* (3), 889–898.
(60) De Smet, K. A.; Weston, A.; Brown, I. N.; Young, D. B.; Robertson, B. D. Three pathways for trehalose biosynthesis in mycobacteria. *Microbiology* **2000**, *146* (1), 199–208.
(61) Woodruff, P. J.; Carlson, B. L.; Siridechadilok, B.; Pratt, M. R.; Senaratne, R. H.; Mougous, J. D.; Riley, L. W.; Williams, S. J.; Bertozzi, C. R. Trehalose is required for growth of *Mycobacterium smegmatis*. *J. Biol. Chem.* **2004**, *279* (28), 28835–28843.
(62) Law, K. F.; Jagirdar, J.; Weiden, M. D.; Bodkin, M.; Rom, W. N. Tuberculosis in HIV-positive patients: cellular response and immune activation in the lung. *Am. J. Respir. Crit. Care Med.* **1996**, *153* (1), 1377–1384.
(63) Islam, N.; Kanost, A. R.; Teixeira, L.; Johnson, J.; Hejal, R.; Aung, H.; Wilkinson, R. J.; Hirsch, C. S.; Toossi, Z. Role of cellular activation and tumor necrosis factor−α in the early expression of *Mycobacterium tuberculosis* 85B mRNA in human alveolar macrophages. *J. Infect. Dis.* **2004**, *190* (2), 341–351.
(64) Singh, G.; Singh, B.; Trajkovic, V.; Sharma, P. *Mycobacterium tuberculosis* 6 kDa early secreted antigenic target stimulates activation of J774 macrophages. *Immunol. Lett.* **2005**, *98* (2), 180–188.
(65) Ryan, L. K.; Golenbock, D. T.; Wu, J.; Vermeulen, M. W. Characterization of proinflammatory cytokine production and CD14 expression by murine alveolar macrophage cell lines. *In Vitro Cell Dev. Biol. Anim.* **1997**, *33* (8), 647–653.
(66) Aung, H.; Toossi, Z.; Wisnieski, J. J.; Wallis, R. S.; Culp, L. A.; Phillips, N. B.; Phillips, M.; Averill, L. E.; Daniel, T. M.; Ellner, J. J. Induction of monocyte expression of tumor necrosis factor alpha by the 30-kD alpha antigen of *Mycobacterium tuberculosis* and synergism with fibronectin. *J. Clin. Invest.* **1996**, *98* (5), 1261–1268.
(67) Trajkovic, V.; Singh, G.; Singh, B.; Singh, S.; Sharma, P. Effect of *Mycobacterium tuberculosis*-specific 10-kilodalton antigen on macrophage release of tumor necrosis factor alpha and nitric oxide. *Infect. Immun.* **2002**, *70* (12), 6558–6566.
(68) Sugawara, I.; Yamada, H.; Kaneko, H.; Mizuno, S.; Takeda, K.; Akira, S. Role of interleukin-18 (IL-18) in mycobacterial infection in IL-18-gene-disrupted mice. *Infect. Immun.* **1999**, *67* (5), 2585–2589.
(69) Kindler, V.; Sappino, A. P.; Grau, G. E.; Piguet, P. F.; Vassalli, P. The inducing role of tumor necrosis factor in the development of bactericidal granulomas during BCG infection. *Cell* **1989**, *56* (5), 731–740.
(70) Byrd, T. F. Tumor necrosis factor−a (TNF-a) promotes growth of virulent *Mycobacterium tuberculosis* in human monocytes: iron-mediated growth suppression is correlated with decreased release of TNF-a from iron treated infected monocytes. *J. Clin. Invest.* **1997**, *99* (10), 2518–2529.
(71) Engele, M.; Stossel, E.; Castiglione, K.; Schwerdtner, N.; Wagner, M.; Bolcskei, P.; Rollinghoff, M.; Stenger, S. Induction of TNF in human alveolar macrophages as a potential evasion mechanism of virulent *Mycobacterium tuberculosis*. *J. Immunol.* **2002**, *168* (3), 1328–1337.
(72) Liew, F. Y.; Cox, F. E. Nonspecific defense mechanism: the role of nitric oxide. *Immunol. Today* **1991**, *12* (3), 17–21.
(73) Holland, S. M. Host defense against nontuberculous mycobacterial infections. *Semin. Respir. Infect.* **1996**, *11* (4), 217–230.
(74) Fujiwara, H.; Kleinhenz, M. E.; Wallis, R. S.; Ellner, J. J. Increased interleukin-1 production and monocyte suppressor cell activity associated with human tuberculosis. *Am. Rev. Respir. Dis.* **1986**, *133* (1), 73–77.
(75) Fremond, C. M.; Togbe, D.; Doz, E.; Rose, S.; Vasseur, V.; Maillet, I.; Jacobs, M.; Ryffel, B.; Quesniaux, V. F. IL-1 receptor-mediated signal is an essential component of MyD88-dependent innate response to *Mycobacterium tuberculosis* infection. *J. Immunol.* **2007**, *179* (2), 1178–1189.
(76) Akira, S.; Kishimoto, T. Contribution of IL-18 to Th1 response and host defense against infection by *Mycobacterium tuberculosis*: a comparative study with IL-12p40. *Immunol. Rev.* **1992**, *127*, 25–50.
(77) Kishimoto, T.; Akira, S.; Taga, T. Interleukin-6 and its receptor: a paradigm for cytokines. *Science* **1992**, *258* (5082), 593–597.
(78) Kopf, M.; Baumann, H.; Freer, G.; Freudenberg, M.; Lamers, M.; Kishimoto, T.; Zinkernagel, R.; Bluethmann, H.; Kohler, G. Impaired immune and acute-phase responses in interleukin-6-deficient mice. *Nature* **1994**, *368* (6469), 339–342.
(79) Ladel, C. H.; Blum, C.; Dreher, A.; Reifenberg, K.; Kaufmann, S. H. Protective role of gamma/delta T cells and alpha/beta T cells in tuberculosis. *Eur. J. Immunol.* **1995**, *25* (10), 2877–2881.
(80) Kinjo, Y.; Kawakami, K.; Uezu, K.; Yara, S.; Miyagi, K.; Koguchi, Y.; Hoshino, T.; Okamoto, M.; Kawase, Y.; Yokota, K.; Yoshino, K.; Takeda, K.; Akira, S.; Saito, A. Contribution of IL-18 to Th1 response and host defense against infection by *Mycobacterium tuberculosis*: a comparative study with IL-12p40. *J. Immunol.* **2002**, *169* (1), 323–329.
(81) Biet, F.; Kremer, L.; Wolowczuk, I.; Delacre, M.; Locht, C. *Mycobacterium bovis* BCG producing interleukin-18 increases antigen-specific gamma interferon production in mice. *Infect. Immun.* **2002**, *70* (12), 6549–6557.
(82) Gudmundsson, G.; Hunninghake, G. W. Interferon-gamma is necessary for the expression of hypersensitivity pneumonitis. *J. Clin. Invest.* **1997**, *99* (10), 2386–2390.
(83) Nathan, C. F.; Hibbs, J. B., Jr. Role of nitric oxide synthesis in macrophage antimicrobial activity. *Curr. Opin. Immunol.* **1991**, *3* (1), 65–70.

PR8009462